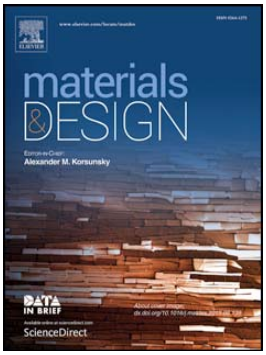


# Phenomenological characterization of sequential dual-curing of off-stoichiometric "thiol-epoxy" systems: Towards applicability

Alberto Belmonte, Xavier Fernández-Francos, Àngels Serra, Silvia De la Flor

PII: S0264-1275(16)31300-4
DOI: doi: 10.1016/j.matdes.2016.10.009
Reference: JMADE 2366

To appear in:

Received date: 30 August 2016
Revised date: 4 October 2016
Accepted date: 5 October 2016

Please cite this article as: Alberto Belmonte, Xavier Fernández-Francos, Àngels Serra, Silvia De la Flor, Phenomenological characterization of sequential dual-curing of off-stoichiometric "thiol-epoxy" systems: Towards applicability, (2016), doi: 10.1016/j.matdes.2016.10.009

# Phenomenological characterization of sequential dual-curing of off-stoichiometric "thiol-epoxy" systems: Towards applicability

**Alberto Belmonte [1], Xavier Fernández-Francos [2], Àngels Serra[3], Silvia De la Flor [1,*]**

1) Department of Mechanical Engineering, Universitat Rovira i Virgili, Av. PaïsosCatalans 26, 43007, Tarragona, Spain; albertofrancisco.belmonte@urv.cat
2) Thermodynamics Laboratory, ETSEIB, Universitat Politècnica de Catalunya, Av. Diagonal 647, 08028, Barcelona, Spain; xavier.fernandez@mmt.upc.edu
3) Department of Analytical and Organic Chemistry, Universitat Rovira i Virgili, C/Marcel·lí Domingo s/n, 43007, Tarragona, Spain; angels.serra@urv.cat

* Correspondence: silvia.delaflor@urv.cat; Tel.: +34-977558839; Fax: +34-977559602

## Abstract

An extensive characterization of a sequential dual-curing system based on off-stoichiometric "thiol-epoxy" mixtures was carried out using thiol compounds of different functionality. The intermediate and final materials obtained after each curing stages at different thiol-epoxy ratios were studied by means of thermomechanical and rheological experiments. The storage and loss modulus and the loss factor *tan δ* were monitored during the curing process to analyse gelation and network structure build-up. The critical ratio for gelation was determined making use of the ideal Flory-Stockmayer theory and compared with experimental results. Intermediate materials obtained in the vicinity of the theoretical critical ratio did not have the mechanical consistency expected for partially crosslinked materials, did not retain their shape and even experienced undesired flow upon heating to activate the second curing reaction. The rheological results showed that the critical ratio is higher than the predicted value and that a softening during the second curing stage affects the shape-retention at this ratio. From the thermomechanical results, a wide range of intermediate and final materials with different properties and applicability can be obtained by properly choosing the thiol-epoxy ratio: from liquid-like to highly deformable intermediate materials and from moderately crosslinked (deformable) to highly crosslinked (brittle) final materials.

## Keywords

Dual-curing; thiol-epoxy; functional materials; rheological analysis; thermo-mechanical analysis

## 1. Introduction

Crosslinked polymeric materials (thermosets) are used in many application fields because of their excellent thermal and mechanical properties (i.e. aviation, automobile, structures or coatings) [1]. The possibility of forming network structures with tuneable properties and the presence of reversible network relaxation processes make them suitable materials for more demanding applications such as self-healing materials, optical devices or lithographic printing [2,3]. Nowadays, the increasing demand of smart materials with complex shape designs (i.e.

aircraft pieces, bio-inspired devices or shape-changing materials [4]), has become a great challenge for thermosets because accurate control of the curing process is necessary to fit the complex processing [5]. The formation of crosslinked network structures is a non-reversible process involving drastic changes in polymer and network structure with tight time-temperature constraints that need to be carefully controlled in order to produce components with required shapes and properties in complex processing scenarios. Recently, a new concept in crosslinking processes based on the sequential combination of two polymerization processes (dual-curing processing) has come out as an interesting and versatile approach for better controlling of the network structure build-up and properties during processing [6-8].

Dual-curing systems arise from the combination of two compatible and well-controlled polymerization processes taking place simultaneously [9,10] or sequentially [11]. Sequential dual-curing has the advantage of forming an intermediate and stable material after the first polymerization process which is further transformed into the final material after the second polymerization process. This is commonly achieved by combination of polymerization processes triggered by different stimuli, such as UV-light and heat, or else has sufficiently different reaction kinetics. Examples of such processes include photo-curing/thermal-curing click thiol-ene/thiol-epoxy systems [11], aza-Michael addition/free-radical polymerization of amine-acrylate systems [12] and both photo-curing thiol/ene/cationic systems [13].

Click reactions are based on efficiency, versatility and selectivity [14-16], a combination of features that makes them suitable for dual-curing processing [11]. In particular, “thiol-click” reactions are highly interesting because they can react at mild conditions producing radical or anionic species in a controlled and efficient manner by appropriately choosing the catalyst [17-19]. Among them, the thiol-epoxy click reaction, a step-wise reaction mechanism catalysed by tertiary amines, which consists essentially in the nucleophilic attack to the oxirane ring by the thiolate anion, produces functional soft materials with excellent mechanical properties (high resistance and elongation at break) that can be useful in a first-stage life as shape-memory polymers (i.e. for size reduction in transport or storage processes) and further transform into new polymeric structures [20-22]. In our previous work [23], a new sequential dual-curing system based on off-stoichiometric thiol-epoxy mixtures with epoxy excess catalysed by tertiary amines was presented. The combination of the thiol-epoxy click reaction followed by the homopolymerization of the epoxy excess produces two-stage materials with tuneable thermomechanical and structural properties with the advantage of a single-pot reaction mechanism. Dual-curing processing is achieved in this case by the kinetics control of both curing reactions: the thiol-epoxy addition takes place rapidly at low temperature while the epoxy homopolymerization remains almost latent due to the slow kinetics at this temperature [24-27]. The intermediate and final material properties depend on the functionality and structure of the thiol and epoxy monomers or oligomers and the thiol-epoxy ratio or epoxy excess in the system. In our previous work [23], the network structure build-up during the thiol-epoxy reaction was analysed from a theoretical point of view assuming ideal step-wise behaviour. The critical ratio $r_c$ which defines the minimum thiol-epoxy ratio to form a solid-like and therefore conformable material after the first curing stage was also predicted, a parameter that can be of relevance in the processing of complex shapes. Intermediate and stable materials ranging from highly viscous to solid-like and conformable materials can be obtained after the thiol-epoxy polymerization taking place at low temperature (first curing

process). Hereafter, through an easy mechanically processing, complex shapes can be achieved which are further fixed by the formation of the new network structure caused by the epoxy homopolymerization taking place at higher temperature (second curing process).

In this work, thiol-epoxy dual-curing systems using thiol compounds of different functionality are studied in order to analyse their processing capabilities and the thermomechanical and physical properties of the multifunctional materials obtained. Mixtures at thiol-epoxy ratios below, close and above the critical ratio, $r_c$, were cured and the intermediate and final materials obtained were qualitatively analysed (deformability, consistency, colour, transparency and final shape). Some discrepancies from the theoretical behaviour were found in the processing of materials at the vicinity of $r_c$: the intermediate materials showed excessive deformation and even flow upon heating to activate the second curing reaction when they were not supposed to. The dual-curing process was therefore studied by means of rheological analysis in order to relate the viscoelastic behaviour during curing and, in particular, of the intermediate materials, with the observed behaviour. Relevant viscoelastic parameters such as the storage and loss modulus, and the loss factor $tan\delta$ were monitored at different frequencies. The experimental results were compared with the behaviour expected from the application of the well-known Flory-Stockmayer theory, for ideal step-wise processes, to the thiol-epoxy reaction occurring in the first curing stage. In addition, the thermomechanical and structural properties of the final materials were analysed by means of DMA and the applicability of all materials formed (intermediate and final materials) were discussed in order to optimise the performance of these multifunctional materials.

## 2. Materials and methodology

The epoxy resin diglycidyl ether of bisphenol A (DGEBA, GY240, Huntsman, Everberg, Belgium) with a molecular weight per epoxy equivalent of 182 g/eq was dried at 80ºC under vacuum during three hours prior to use. The curing agents pentaerythritoltetrakis(3-mercaptopropionate) (S4), with a molecular weight per thiol equivalent unit of 122.17 g/equiv and trimethylolpropane tris(3-mercaptopropionate) (S3), with a molecular weight per thiol equivalent unit of 132.85 g/eq (both from Sigma-Aldrich, St. Louis, MO, USA) were used as received and the catalyst 1-methylimidazole (1MI, Sigma-Aldrich, St. Louis, MO, USA) was used as received.

The mixtures were prepared by mixing the compounds in different thiol-epoxy ratios *r* with respect to the epoxy groups. One part per hundred of 1MI of the total mixture (1 phr) was used as catalyst. The mixture was manually stirred in a glass vial and rapidly poured in a Teflon mould. The first curing process was carried out at 50°C during 3 hours to ensure the completion of the thiol-epoxy reaction. Intermediate materials were obtained and the processing of different shapes was carried out using different techniques. Afterwards, the second curing stage was triggered by increasing the temperature up to 120°C (at 5°C/min controlled ramp) and maintaining the oven isothermally during 1 hour at 120°C followed by 1 hour at 150°C to ensure the completion of the epoxy homopolymerization. Final materials with different shapes were obtained.

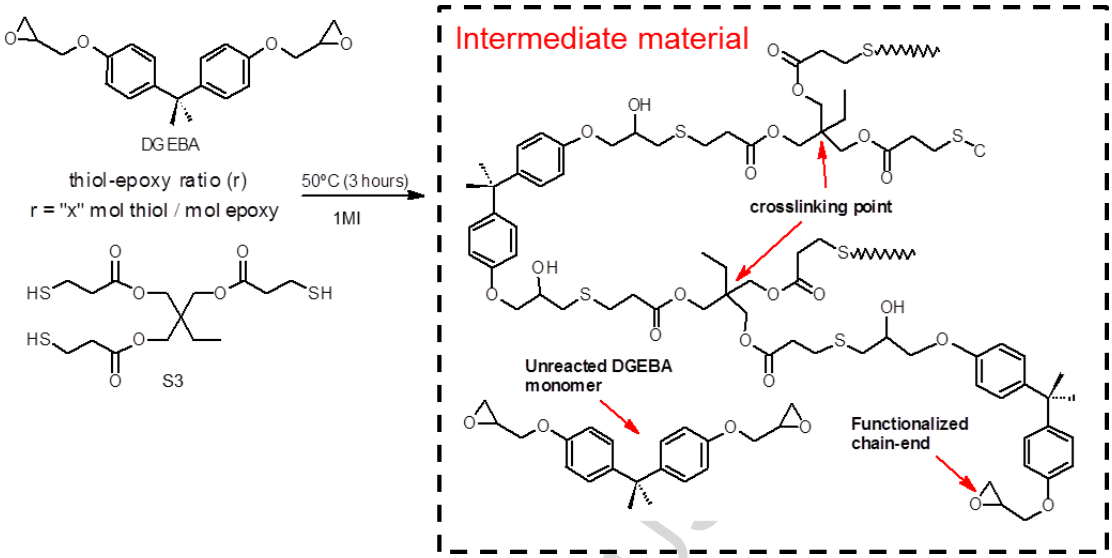


**Figure 1.** Reaction scheme of the first curing stage and expected network structure of the intermediate material in the S3-DGEBAoff-stoichiometric system (thiol-epoxy polymerization)

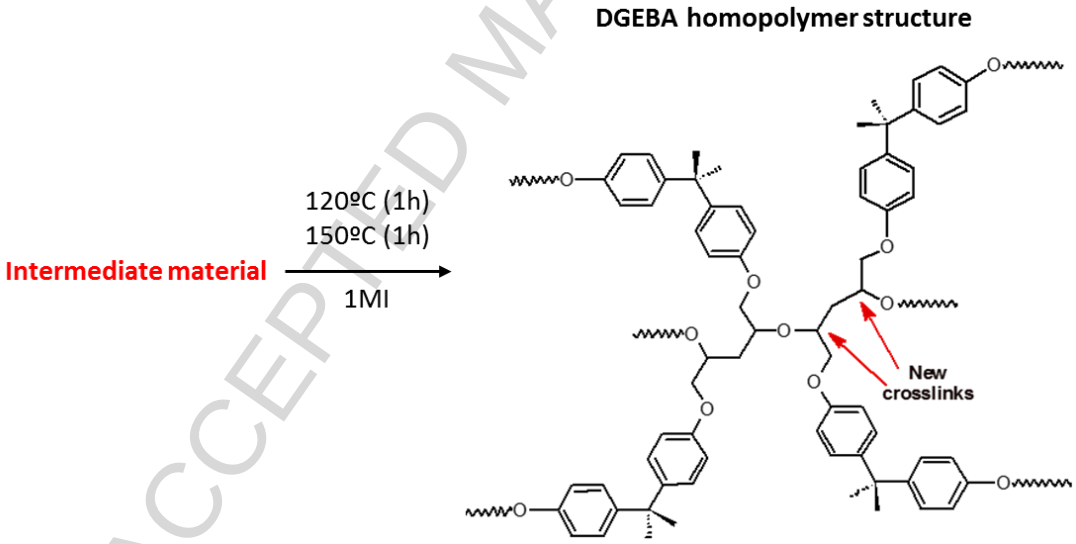


**Figure 2.** Network structure formed after the second curing stage (epoxy homopolymerization)

In Figure 1, the reaction scheme of the first curing process (thiol-epoxy polymerization) and the expected network structure of the intermediate material for a S3-DGEBA formulation is shown. In Figure 2, the new network structure formed after the second curing stage (homopolymerization of the remaining epoxy) is presented.

## 2.1 Theoretical network build-up parameters

As mentioned in the introduction, one of the main advantages on using sequential dual-curing systems is to get an intermediate solid-like and conformable material. To this end, one approach is to define the thiol-epoxy ratio ensuring the gelation takes place during the first curing stage. The gel point conversion can be calculated, assuming ideal step-growth behaviour for the thiol-epoxy reaction, making use of the well-known theory of Flory-Stockmayer:

$$\alpha_{epoxy,gel} = \sqrt{\frac{r_{thiol:epoxy}}{(f_{epoxy}-1)\cdot(f_{thiol}-1)}} \quad (1)$$

In this expression, $\alpha_{epoxy,gel}$ is the conversion of epoxy groups at the gel point, $f_{epoxy}$ and $f_{thiol}$ are the average functionality of epoxy and thiol monomers and $r_{thiol:epoxy}$ is the ratio between thiol and epoxy functional groups. This only produces a valid gel point conversion for values of $r_{thiol:epoxy}$ higher than $r_c$ and lower than $1/r_c$, where $r_c$ is the critical gelation ratio. This parameter can be obtained from the following expression:

$$r_c = \frac{1}{(f_{epoxy}-1)\cdot(f_{thiol}-1)} \quad (2)$$

In the case of formulations with excess of epoxy groups, $r_{thiol:epoxy}$ will be always lower than 1 and therefore only condition for gelation and crosslinking during the first curing stage is that $r_{thiol:epoxy} > r_c$. For lower ratios, the amount of thiol is not sufficient to produce a network during the thiol-epoxy reaction.

## 2.2 Rheological characterization

The dual-curing process was analysed using a rheometer, TA Instruments, New Castle, AR-G2 equipped with an electrical heated plate device (EHP) and parallel plate geometry. Dynamo-mechanical experiments at different frequencies were performed to investigate the evolution of the storage and loss modulus (G' and G'' respectively) during the curing process. The gel point was determined by the crossover of the phase angle δ at different frequencies. The experimental procedure is defined to simulate the curing procedure in the oven: 3 hours at 50°C with oscillation amplitude of 2% (until G' has reached a stable plateau) and of 0.5% (until the end of the curing process). Three different frequencies were continuously measured, from 1 to 10 Hz, 2 points per decade in logarithmic scale (1, 3.16 and 10 Hz). Afterwards, the second curing stage was carried out as follows: a heating rate of 5°C/min from 50 to 120°C followed by 1 hour at 120°C (same oscillation amplitude and frequencies) and 1 hour at 150°C (same oscillation amplitude but only at 1 Hz).

## 2.3 Thermo-mechanical characterization

As in our previous work [23], Fox's law for copolymer networks (see equation (3))can be used to estimate the glass transition temperatures of the intermediate and final materials starting from the experimentally measured values of each component: uncured/cured thiol-epoxy network, uncured/cured epoxy homopolymer network. Such estimation is possible assuming there are no specific interactions between both components [28].

$$\frac{1}{T_{g,m}} = \frac{w_{S-E}}{T_{g,S-E}} - \frac{1-w_{S-E}}{T_{g,E-E}} \quad (3)$$

In equation (3) *w* is the mass fraction and subscripts *S-E* refers to the thiol-epoxy network structure, *E-E* to the epoxy homopolymer network structure, and *m* to the stage of the material (intermediate material, *m*=1, final material, *m*=2). For the intermediate material, $T_{g,E-E}$

is the glass transition temperature of the unreacted DGEBA monomer remaining within the network, while in the final material, $T_{g,E\text{-}E}$ is the glass transition temperature of the DGEBA homopolymer network structure. In both materials, $T_{g,E\text{-}E}$ is the glass transition temperature of the stoichiometric thiol-epoxy network structure.

The $T_{g,S\text{-}E}$ for both, S3 and S4 systems, and the $T_{g,E\text{-}E}$ for both, the intermediate and final materials, were determined by dynamic DSC experiments using a Differential scanning calorimeter Mettler 821e calibrated with indium standards. Neat thiol-epoxy formulations containing S3 or S4 as thiol crosslinker, with $r_{thiol:epoxy}$=1, were used to determine the $T_{g,S\text{-}E}$ of each system. The formulations were cured at 10°C/min from room temperature up to 200°C. A second DSC run at 10 ºC/min up to 120 ºC was performed in order to determine their glass transition temperature. A formulation containing only DGEBA and 1MI was used to determine the $T_{g,E\text{-}E}$ of the intermediate materials, that is, the unreacted DGEBA-1MI mixture, and that of the fully crosslinked material. In this case, the mixture was heated at constant heating rate of 10°C/min from -50°C to 250°C to determine the glass transition of the unreacted mixture and cure completely the material. Afterwards, a second DSC scan was performed at 10 ºC/min from room temperature to 200 ºC to determine the glass transition temperature of the cured material.

In order to verify the predictions made by the Fox equation, dynamic DSC experiments of formulations covering the whole thiol-epoxy ratio ($r_{thiol:epoxy}$ equal to 0.25, 0.5 and 0.75) were performed. The samples were cured in a conventional oven following the procedure explained in the materials section. The intermediate materials were analysed in the DSC at 10°C/min from -50 to 100°C. The final materials were analysed at 10°C/min and from 30 to 200°C.

A DMA Q800, TA Instruments, equipped with a 3-point-bending clamp (15 mm) was used to analyse the thermomechanical and structural properties of the final materials. Oscillatory experiments were carried out at 15 µm of amplitude, 1 Hz of frequency and at a heating rate of 3°C/min from 30°C to 150°C. The glass transition temperature $T_g$ was determined as the peak of the *tanδ* curve, the rubbery modulus ($E_r$) was determined at $T_g$+50°C from the storage modulus curve and the width at half-height (FWHM) and peak value of the *tanδ* curve were determined to further analyse the heterogeneity of the network relaxation process.

## 3. Results and discussion

As stated in previous section, it was decided to analyse the materials with thiol:epoxy ratios in the vicinity of the critical gelation ratio $r_c$; a thiol:epoxy ratio below $r_c$ should lead to uncrosslinked materials with flowing ability at the end of the first curing stage, while a thiol:epoxy ratio above $r_c$ should produce a solid-like and conformable intermediate material. In Table 1 the conversion of epoxy groups at gel $\alpha_{epoxxy,gel}$, calculated using equation (1), and the thiol-epoxy ratio are shown for both, the S3-DGEBA and S4-DGEBA systems. The point at which both, the thiol-epoxy ratio and the conversion are equal (highlighted in intense grey) determine the minimum thiol-epoxy ratio, $r_c$, required to form a gelled material and therefore solid-like and conformable. The exact value for the S4-DGEBA system is $r_c$ =0.333, from equation (2), so $r$=0.35 is only an approximate estimation. As expected, the gel point conversion is lower in systems with higher functionality (S4-DGEBA > S3-DGEBA) for the same

thiol-epoxy ratio because formation of the incipient cross-linked network is easier. Likewise, the critical gelation ratio is also lower.

**Table 1.** Determination of the thiol-epoxy critical ratio for the S3-DGEBA and S4-DGEBA systems

[a]Calculated using equation (1)

| S3-DGEBA | | S4-DGEBA | |
|---|---|---|---|
| **r (thiol-epoxy)** | **$\alpha_{epoxy,gel}$[a]** | **r (thiol-epoxy)** | **$\alpha_{epoxy,gel}$[a]** |
| 0.70 | 0.592 | 0.70 | 0.483 |
| 0.65 | 0.570 | 0.65 | 0.465 |
| 0.60 | 0.548 | 0.60 | 0.447 |
| 0.55 | 0.524 | 0.55 | 0.428 |
| 0.50 | 0.500 | 0.50 | 0.408 |
| 0.45 | 0.474 | 0.45 | 0.387 |
| 0.40 | 0.447 | 0.40 | 0.365 |
| 0.35 | 0.418 | 0.35 | 0.342 |
| 0.30 | 0.387 | 0.30 | 0.316 |

Using the values of the determined $r_c$, intermediate and final materials at $r<r_c$ and $r \geq r_c$ were cured and qualitatively analysed. In Figure 3, pictures of different materials obtained with the S3-DGEBA system are presented. As it can be seen, the intermediate materials are completely transparent and colourless regardless of the thiol-epoxy ratio. Moreover, the transparency remains stable from thin samples (≈ 0.1 mm) to thick samples (> 3 mm). At $r<r_c$, high viscous and sticky materials were obtained, whereas on increasing the ratio up to $r_c$, solid-like and highly deformable materials were obtained (Figure 3a). At thiol:epoxy ratios far above $r_c$, hardly deformable intermediate materials are obtained due to the higher content of thiol-epoxy network structure. After the second curing stage (Figure 3b), the final materials remains transparent but colour changes are appreciated. The anionic epoxy homopolymerization leads to intense brown materials due to the presence of initiator fragments with conjugated double bonds in chain ends [26]. As a consequence, decreasing the thiol-epoxy ratio (higher epoxy excess), leads to darker samples. This is interesting from a qualitative point of view because only through the colour of the sample, one can deduce the amount of epoxy excess present in the material, and also from the application point of view, depending on whether colour is important or not. All the final materials were rigid at room temperature and those formulations containing higher epoxy excess, $r<r_c$, showed higher fragility. This was proved during the sample release from the curing mould: various samples with higher content of epoxy excess broke due to the force applied. The formation of a high densely network structure by the anionic epoxy polymerization leads to brittle materials [29].

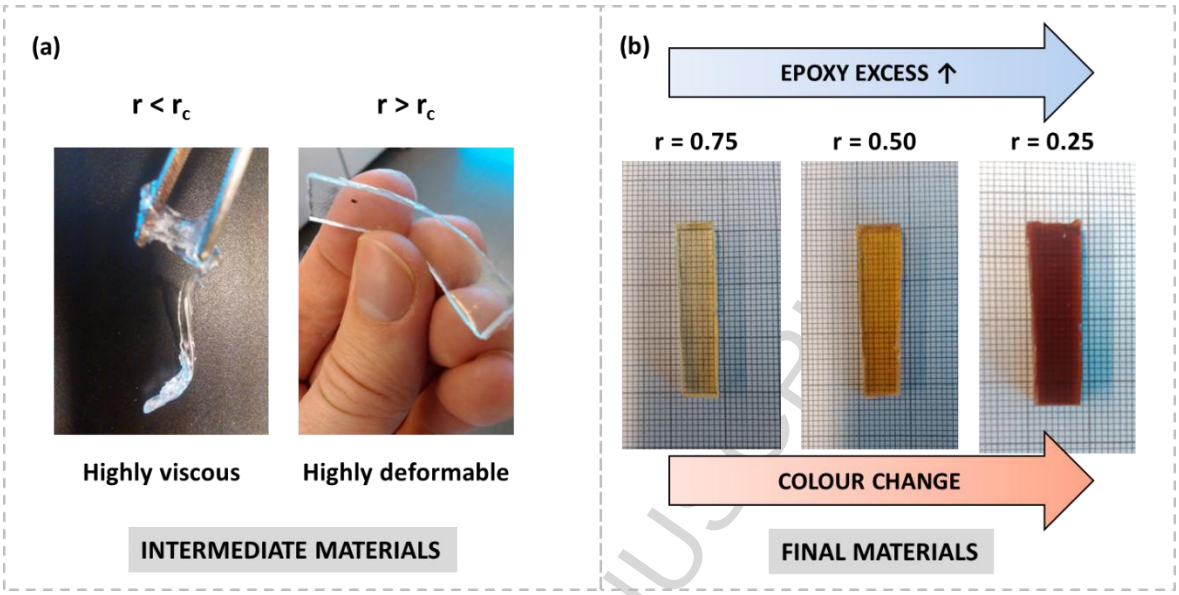


**Figure 3.** Examples of different intermediate and final materials obtained at different thiol-epoxy ratios

In Figure 4 some examples of conformation and processing of complex shapes are shown using formulations with ($r>r_c$). As it can be seen, choosing an appropriate thiol:epoxy ratio makes it possible to form a solid-like and conformable material. This intermediate material (i.e. a thick-type or film-type material) can be deformed into a spring, bent or other complex and uncommon shape through a mechanical or even manual processing. Afterwards, these shapes can be fixed through the second curing stage. Nevertheless, because of the low $T_g$ ($T_g<T_{room}$), viscoelastic relaxation is fast, leading to a recovery of the original shape when temperature starts to increase for the activation of the second curing stage. Therefore, in order to fix the shape, it is necessary to constrain this shape during the heating and subsequent curing. Therefore, complex shapes were successfully achieved, and no cracking was appreciated over the surface due to shrinkage and internal stresses generated during the epoxy homopolymerization process [30].

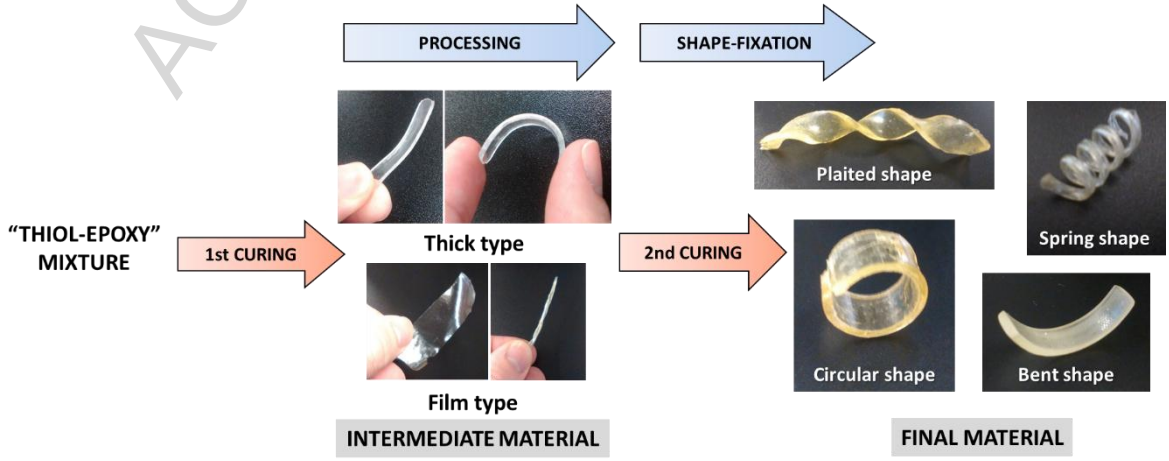


**Figure 4.** Examples of shape-processing (intermediate material) and shape-fixation (final material)

Taking advantage of this process, it is possible to obtain well-defined circular-shapes for structural applications such as opening and closing mechanisms (shape-memory actuators

[31]), or otherwise forming complex shape designs (i.e. a plaited-shape or bent-shape) for more demanding applications. In addition, using film-type samples it is possible the processing of long wires by rolling it up and further develop spring-shaped final materials. Moreover, the film-type materials are valuable for bonding pipes or coating purposes because the film can be easily adapted to different types of shapes and elongated as desired.

Nevertheless, as mentioned in the introduction, the imposed final shape is not well-retained when the thiol-epoxy ratio is too close to $r_c$. The advantage on using these formulations is the enhanced deformability caused by the low modulus and $T_g$ achieved after the first curing stage. In Figure 5, the curing of a spring-shaped material using the formulation S3-DGEBA-0.55 (note that $r_c$ is 0.5) is shown. As it can be seen, the shape is lost but, unexpectedly, it was also observed significant dripping, indicative of a liquid-like behaviour. The situation was similar for both S3-DGEBA and S4-DGEBA systems at stoichiometric ratios slightly above $r_c$.

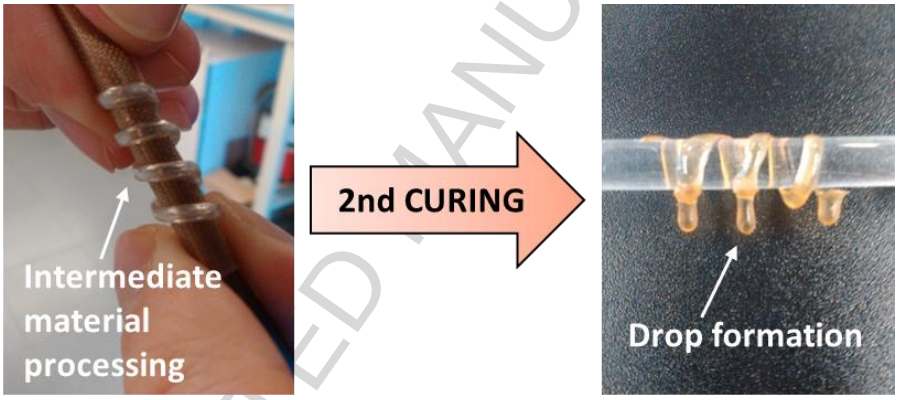


**Figure 5.** Example of the shape-losing after the second curing stage in a formulation with a thiol-epoxy ratio close to the critical ratio (S3-DGEBA-0.55)

Taking into account the above results, an experimental scenario was set up to analyse in depth this phenomenon (from here and so on, we will refer to this phenomenon as “dripping” behaviour). In Figure 6, a scheme of the “dripping test” methodology is shown. Different partially cured specimens with $r \geq r_c$ were suspended vertically from one end. This way, elongation is only due to its own weight. Afterwards, the second curing stage is triggered following the same procedure explained in the materials and methods section. Finally, the dripping suffered in the different specimens is qualitative and/or quantitative analysed. It is of key importance to ensure that all the specimens have the same dimensions, thus they were carefully cured in order to obtain the same sizes, 30 x 6 x 1.5 $mm^3$. In order to further analyse each section of the specimen separately, various equidistant marks were painted along the specimens. As it can be seen in Figure 6, the marked specimens were held by the top-side with minimal force onto a Teflon surface in order to avoid the sample being flattened during the experiment.

The dripping behaviour was qualitatively and, when possible, quantitatively analysed through equation (4) (which quantifies the % of elongation suffered during the second curing stage).

$$Dripping(\%) = \frac{\Delta_{l,tot}}{l_0} \cdot 100 \quad (4)$$

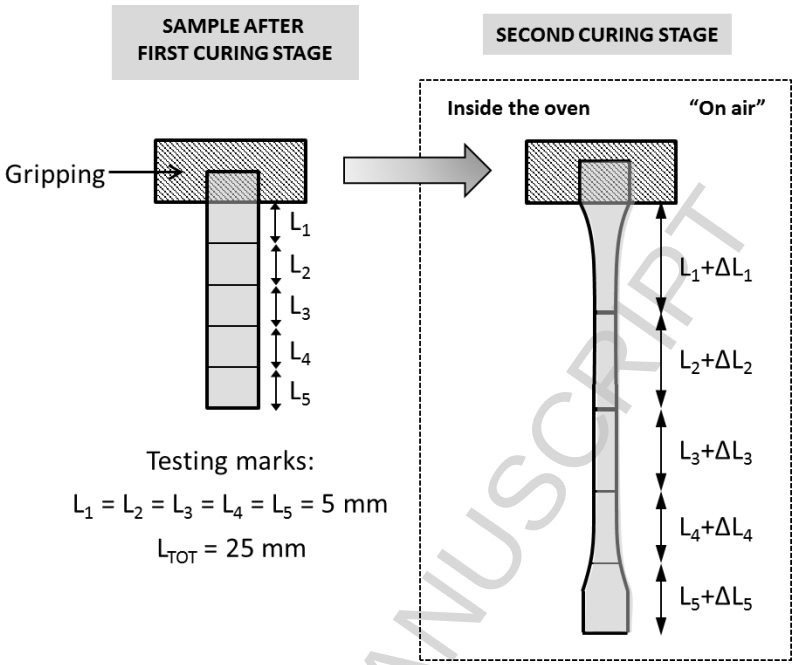


**Figure 6.** Dripping test scenario: on the left side the specimen marked and measured before testing; on the right side the elongation suffered after the second curing stage. All the measured parameters have been highlighted.

In Table 2, the results of the dripping test are summarized for the S3-DGEBA and S4-DGEBA systems. The symbol ∞ means that the entire sample fell off the support during the experiment. As it can be seen, both formulations stop dripping at $r = r_c + \approx 0.15$ (considering a % of dripping < 2% as the "no-dripping" point). In Figure 7, examples of the dripping test for the S3-DGEBA and S4-DGEBA systems are shown. Overall, samples with ratios close to $r_c$ broke at the fastening point and completely fell off (see S4-DGEBA-0.35 and S3-DGEBA-0.50), whereas with increasing the ratio, the sample did not break but showed high elongation (see S3-DGEBA-0.60). Finally, at a certain ratio (S3-DGEBA-0.65 and S4-DGEBA-0.5), the sample completely retained the shape (no-dripping ratio $r_d$). According to the theoretical model based on ideal step-wise behaviour [23], the crosslinking density of formulation S3-DGEBA-0.60 was about one-two orders of magnitude lower than that of the stoichiometric material S3-DGEBA-1.0 and it means that it should have a modulus in the range of hundreds of kPa, which should be more than enough to maintain the shape; however, the sample showed high elongation pointing out some discrepancies from the theoretical behaviour.

**Table 2.**Dripping test: quantitative results

| Formulation | $L_0$ | $\Delta l_1$ | $\Delta l_2$ | $\Delta l_3$ | $\Delta l_4$ | $\Delta l_5$ | $\Delta l_{,total}$ | Dripping (%) |
|---|---|---|---|---|---|---|---|---|
| **S3-DGEBA-0.50** | 25 | ∞ | ∞ | ∞ | ∞ | ∞ | ∞ | ∞ |
| **S3-DGEBA-0.55** | 25 | ∞ | ∞ | ∞ | ∞ | ∞ | ∞ | ∞ |
| **S3-DGEBA-0.60** | 25 | 4 | 3 | 2 | 1 | 0 | 12 | 48 |
| **S3-DGEBA-0.65** | 25 | 0.2 | 0.1 | 0 | 0 | 0 | 0.3 | 1.2 |
| **S4-DGEBA-0.35** | 25 | ∞ | ∞ | ∞ | ∞ | ∞ | ∞ | ∞ |
| **S4-DGEBA-0.40** | 25 | ∞ | ∞ | ∞ | ∞ | ∞ | ∞ | ∞ |
| **S4-DGEBA-0.45** | 25 | ∞ | ∞ | ∞ | ∞ | ∞ | ∞ | ∞ |
| **S4-DGEBA-0.50** | 25 | 0 | 0 | 0 | 0 | 0 | 0 | 0 |

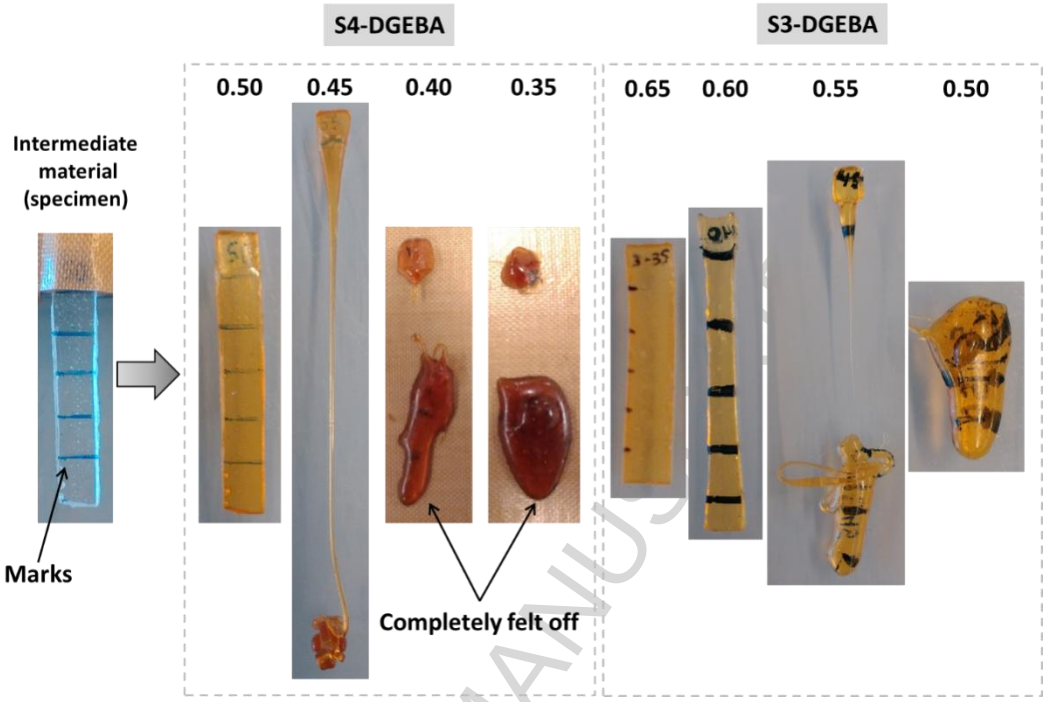


**Figure 7.** In the left side, the specimen of assay (sized and marked intermediate material) and in the right side, the specimens after the dripping test in both systems.

In order to rule out any possible heterogeneity of the samples, DSC analysis were carried out in different parts of the specimen using the same experimental procedure as explained in the materials and methodology section (in this case from 30°C to 120°C). The $T_g$ values in Table 3 indicate all the formulations were homogeneous regardless of the dripping; the $T_g$ values obtained are almost equal in any part of the specimens.

**Table 3.** Glass transition nominal values obtained from DSC tests of those specimens showing dripping behaviour. Experiments were performed in different sections of the specimen: upper, middle and lower side.
[(a)]The sample completely fell off, two separated pieces were extracted and analysed. [(b)]The sample reached the floor, the middle section was mixed with the lower part.

| Formulation | $T_{g,2}$ (DSC) (Upper) | $T_{g,2}$ (DSC) (Middle) | $T_{g,2}$ (DSC) (Lower) | $T_{g,2}$ (DSC) (Average) |
|---|---|---|---|---|
| **S3-DGEBA-0.50** | 73.7 - 72.1[(a)] | | | 72.9 |
| **S3-DGEBA-0.55** | 70.1 - 69.8[(a)] | | | 70.0 |
| **S3-DGEBA-0.60** | 65.9 | 65.6 | 66.1 | 65.9 |
| **S4-DGEBA-0.35** | 102.2 - 100.3[(a)] | | | 101.3 |
| **S4-DGEBA-0.40** | 94.5 - 95.3[(a)] | | | 94.9 |
| **S4-DGEBA-0.45** | 92.2 | ---[(b)] | 91.6 | 91.9 |

Given that the samples were homogeneous from the structure point of view, it was hypothesized that the assumption of ideal step-wise behaviour for the thiol-epoxy reaction may not be realistic at all. Some of the samples showed a flow-like behaviour, as if they were not gelled, when they should not, indicating that gelation might have been delayed. In

consequence, rheological tests were therefore carried out in order to understand the observed behaviour.

## 3.1 Rheology analysis

In basis of the results obtained in the previous section, the rheological analysis of the dual-curing process can provide useful information about the viscoelastic properties of the materials in relation with the dripping phenomenon observed. Two different formulations of each system were analysed: one in which no dripping was appreciated (S3-DGEBA-0.65 and S4-DGEBA-0.50) and one in which "∞" dripping was shown (S3-DGEBA-0.55 and S4-DGEBA-0.40, in both formulations the sample completely fell off). In Figure 8, the entire curing process for the S3-DGEBA-0.55 is presented. In order to follow-up the evolution of the curing process, both the storage modulus (*G'*) and loss modulus (*G''*) at different frequencies are represented against the global time of the experiment (*t*). In addition, the temperature profile during the experiment is shown. As it can be observed, the evolution of the curing process is frequency dependent until the material is completely cured (*t*> 200 min). During polymerization, the material passes through different phases: from a liquid-like material, where both *G'* and *G''*, as well as $tan\delta$ (the loss factor) are frequency-dependent, up to the formation of a solid-like elastic material where *G'* becomes independent of the frequency and *G'*>>*G''* ($tan\delta \approx 0$, elastic mechanical response). During the first curing stage (three hours at 50°C), the thiol-epoxy polymerization takes place within the first 30-40 minutes because of the drastic increase in both, *G'* and *G''*, of about 4 orders of magnitude followed by a stable plateau, in agreement with the previous kinetics analysis [23]. Afterwards, *G'* slightly increases with the time, because of the epoxy homopolymerization taking place slowly at this temperature [23]. During the temperature increase from 50°C to 120°C in the second curing stage, both *G'* and *G''* decrease to a certain extent indicating a softening of the material due to the increasing temperature. Finally the epoxy homopolymerization takes place with a drastic increase in *G'* up to values in the range of MPa while *G''* remains at values two orders of magnitude lower, indicating elastic mechanical response ($tan\delta \approx 0$), and frequency independence.

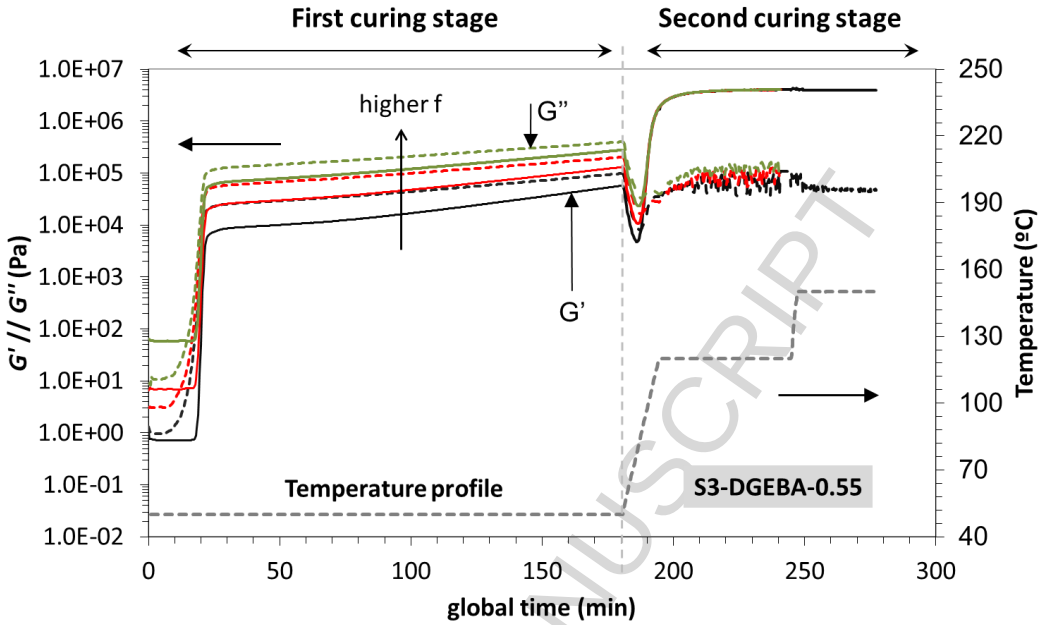


**Figure 8.** Storage modulus (*G’*), loss modulus (*G’’*), and the temperature profile is shown for the whole dual-curing process in the S3-DGEBA-0.55 formulation**.**

As mentioned above, one of the possible reasons explaining the dripping behaviour is the wrong determination of the gel point from equation (1). The gelation process is frequency-independent and therefore, the most consistent gelation criterion is the crossover of *tanδ* curves at different frequencies [34] or, equivalently, the crossover of the phase angle *δ*. In Figure 9, the phase angle (*δ*) is represented in front of the time during the first curing stage. A typical maximum in *δ* or *tanδ* during curing is observed before gelation takes place, because the increase in molecular weight produces an increase in viscosity and therefore in the loss modulus *G’’*, while the elastic component *G’* is hardly affected. Then the phase angles start to decrease due to the increase in *G’* and, if gelation takes place, a crossover takes place. As it can be seen, in formulations where maximum dripping was shown (S3-DGEBA-0.55 and S4-DGEBA-0.40), the crossing of *δ* is not appreciated and therefore the intermediate material formed is not gelled yet. This confirms that network build-up during curing of thiol-epoxy formulations does not follow an ideal step-wise behaviour, and therefore the predictions made using the ideal Flory-Stockmayer expressions are inaccurate. By way of contrast, in formulations where no dripping was shown (S3-DGEBA-0.65 and S4-DGEBA-50), the crossover of *δ* is clearly appreciated pointing out the formation of a gelled network structure.

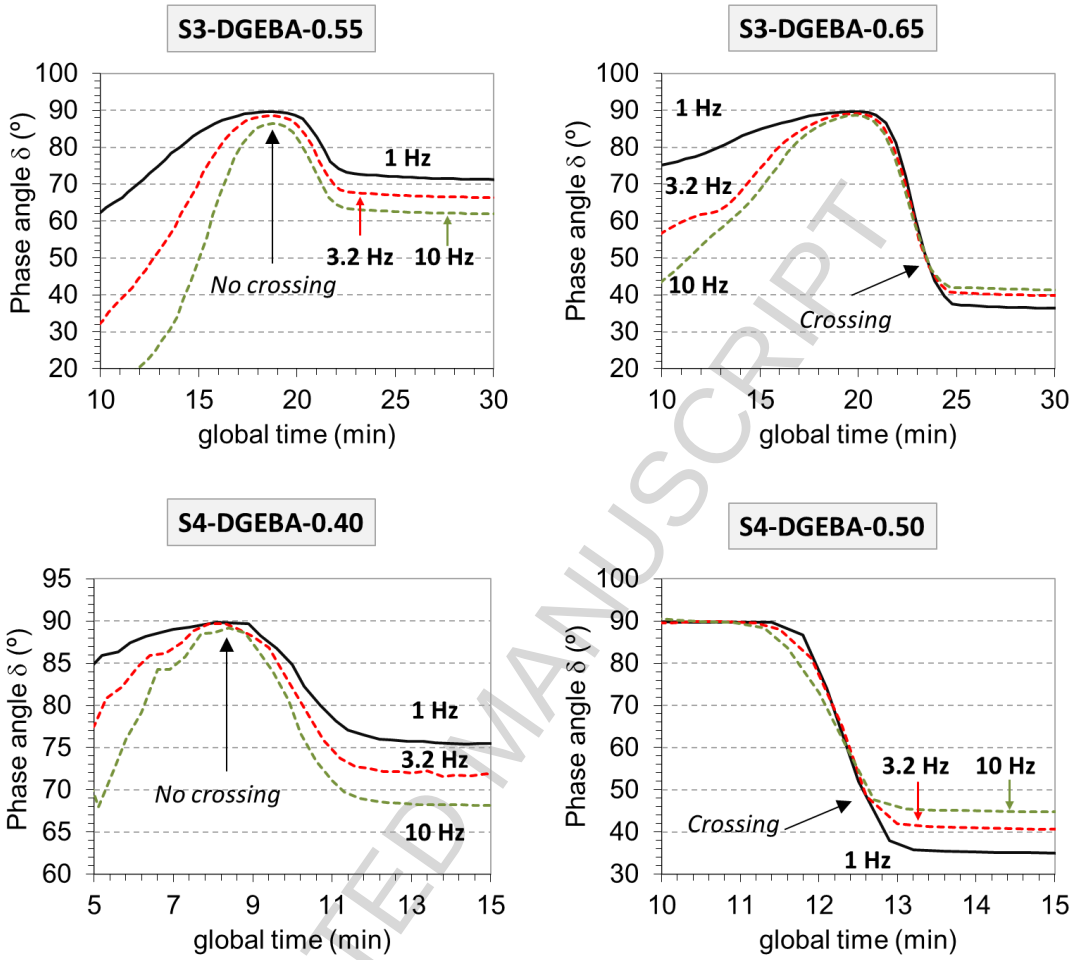


**Figure 9.** Phase angle ($\delta$) against the experiment global time for all the formulations of study. The crossing of the curves has been highlighted**.**

In Figure 10, $\delta$ is represented against the temperature during the temperature increase from 50°C to 120°C for those formulations where no gelation took place in the first curing stage. As it was expected, gelation takes place during the early stage of the second curing process. This may explain why the samples completely fell off during the dripping test: the lack of network structure and the softening of the samples (see the decrease in modulus in Figure 8) enable the sample to flow as a highly viscous liquid until the shape is completely lost, before the second curing process is activated and the material starts to build-up a network structure.

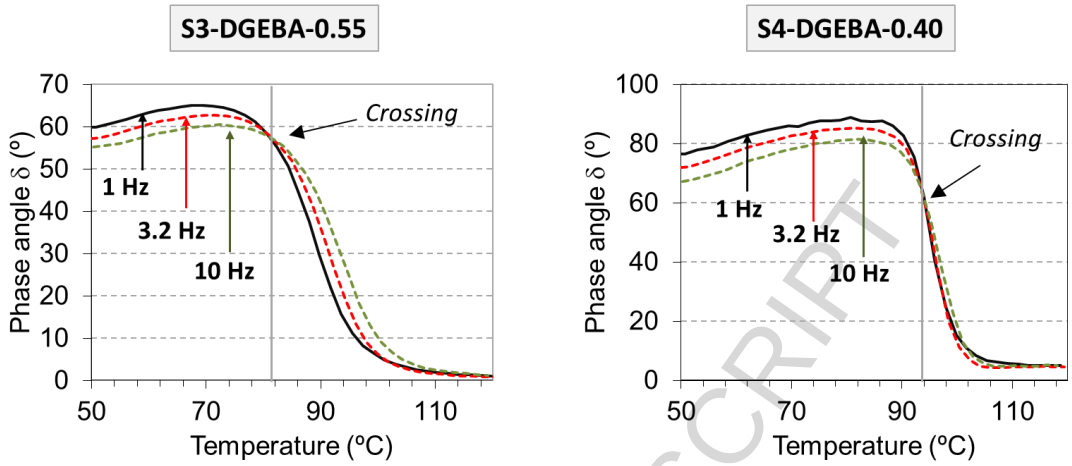


**Figure 10.** Phase angle ($\delta$) against the temperature for the S3-DGEBA-0.55 and S4-DGEBA-0.40 formulations during the temperature increase (50ºC to 120º) in the second curing stage. The crossing of the curves has been highlighted.

In Figure 11, the evolution of *G'* and *G''* during the temperature increase is represented. In formulations where gelation takes place in the first curing stage (S3-DGEBA-0.65 and S4-DGEBA-0.40), *G'* is already above or rapidly overpasses *G"* at low temperature (50-60°C). On the contrary, formulations without gelled structure have higher *G''* until 80-100°C, when gelation takes place and the material starts to build-up a network structure with a more elastic character. In the ungelled formulations (S3-DGEBA-0.55 and S4-DGEBA-0.4), the modulus decreases about 1-2 orders of magnitude upon heating due to the softening of the highly viscous structure, reaching values as low as 30 Pa at 1 Hz in the case of the S4-DGEBA-0.40 formulation. This significant change can explain the elongation and flow (the samples are liquid-like) of the sample because of its own weight in the previous experiments. In the case of S3-DGEBA-0.55 the modulus at 1 Hz decreases only down to 5 kPa but, given that the characteristic timescale during the "dripping" experiment may be in the range of minutes, a measurement in the range of 0.01 Hz would lead to an even lower modulus and also explain the considerable elongation and flow observed. In contrast, formulations with already gelled structure (S3-DGEBA-0.65 and S4-DGEBA-0.5) have *G'* values around or above 0.1 MPa, sufficiently high to avoid sample elongation. The explanation of those formulations that elongated but not completely fell down (i.e. S3-DGEBA-0.60) during the dripping test is probably a matter of time. Following the same reasoning as above, the intermediate material is probably not gelled after the first curing stage, making it possible to elongate the sample due to the softening of the material. However, gelation takes place in the early stage of the second curing process, therefore quickly building up a crosslinked structure preventing further elongation.

From this preliminary analysis, it appears that the effective critical ratio for the S3-DGEBA system should be close to 0.65, and for the S4-DGEBA system should be close to 0.50, and not 0.5 and 0.33 as it is predicted by the Flory-Stockmayer theory. Such departures from the ideal step-wise behaviour are commonly explained by negative substitution effects, which is unlikely in the present case, or better intramolecular cyclization [32, 33]. Intra-molecular cyclization would lead to a delayed gel point conversion, a looser network structure with larger deformability, and leading in some cases to no gelation at all and a lack of network structure [34]. On the other hand, the curing agents S3 (purity>95%) and S4 (purity>95%) were used as

received, and the presence of impurities may result in a lower thiol functionality, hence leading to higher conversion at gelation and looser network structure. A further detailed analysis of gelation and network build-up is out of the scope of this work. Combined calorimetric, rheological and thermomechanical experiments, as well as solubility measurements, are being done and preliminary results confirm the displacement of the gelation to higher conversion accordingly to the explanation given above. The results of this more detailed analysis will be subject of a future work.

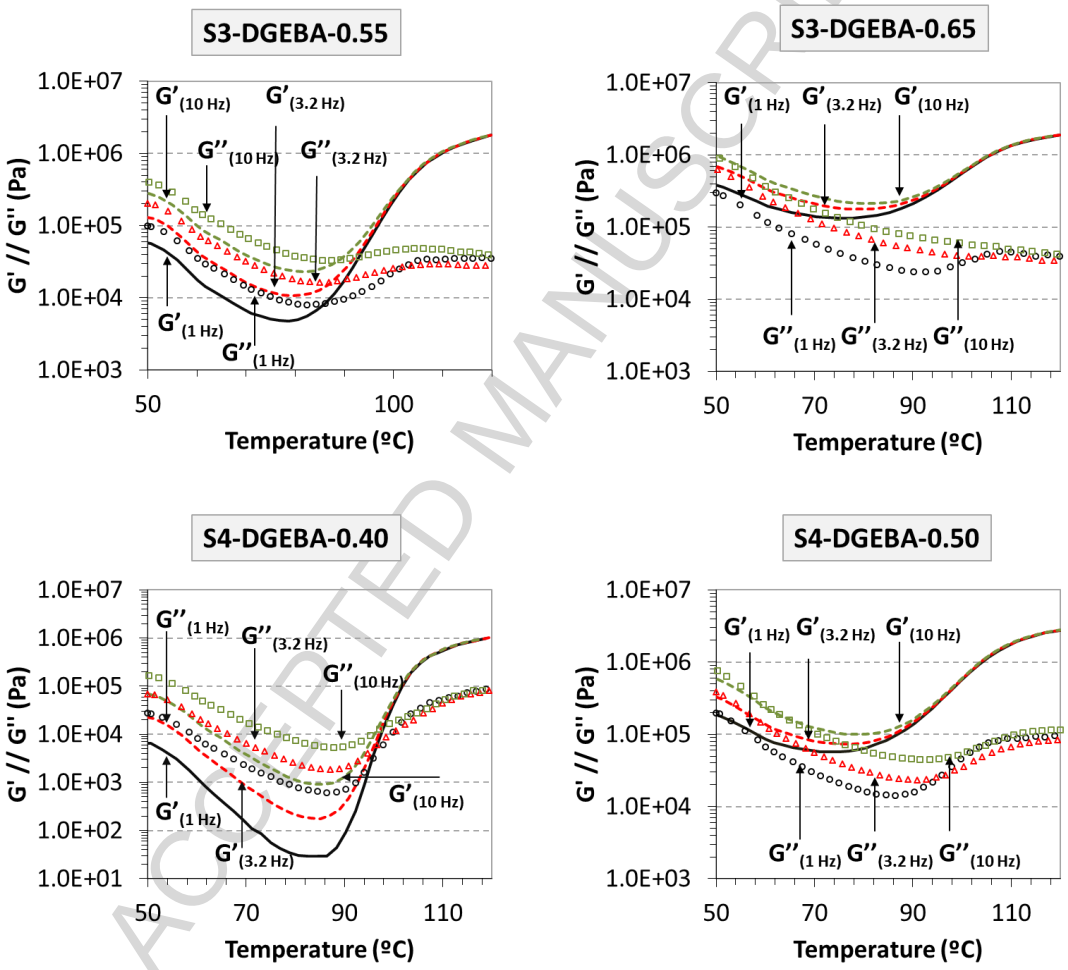


**Figure 11.**Loss modulus (*G''*) and storage modulus (*G'*) during the temperature increase in the second curing stage for all the formulations of study.

## 3.2 Thermo-mechanical characterization towards applicability

In this section, the thermo-mechanical and structural properties of the different formulations of study are shown in order to evaluate the intermediate and final materials with respect to the potential applicability. In Figure 12, the predicted values of $T_{g,1}$ and $T_{g,2}$ (intermediate and final materials) at the different thiol-epoxy ratios (continuous lines) and the experimental values determined by DSC analysis (points) are represented. The apparent critical ratio, determined from the "dripping" experiments ($r_d$) has also been included, in order to divide the graphic in different sections (A and B) accordingly to the physical state of the sample after each curing stage, liquid-like or solid-like.

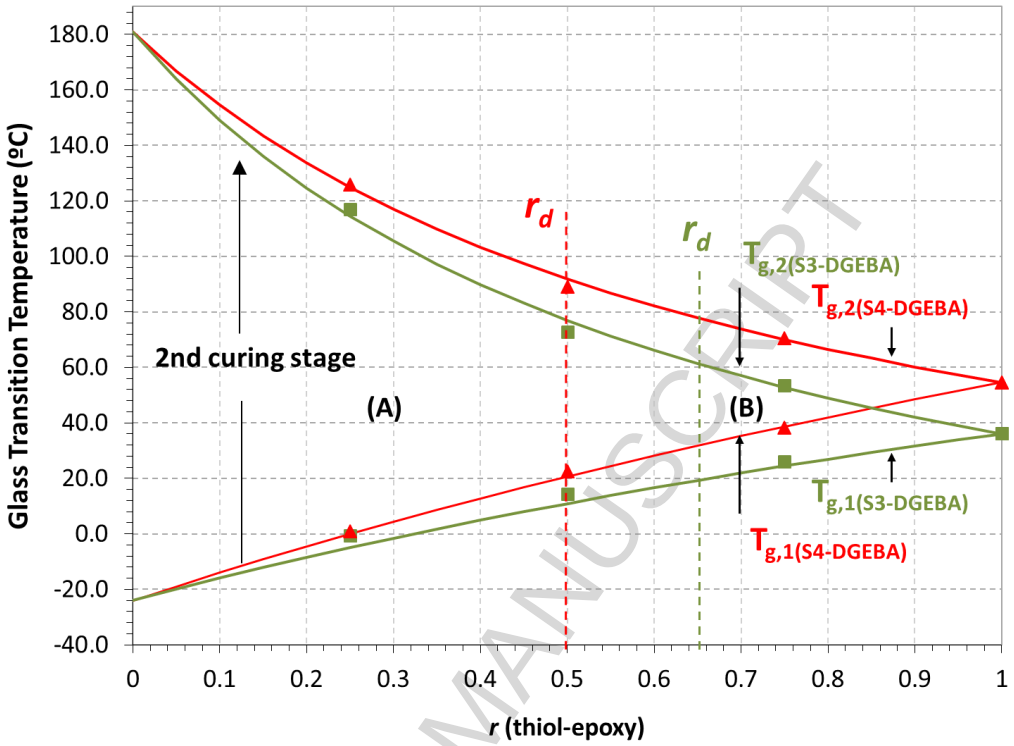


**Figure 12.**Glass transition temperatures and the apparent thiol-epoxy critical ratio of S3 and S4 systems against the thiol-epoxy ratio: comparison between predicted and experimental values.

As it can be observed, the DSC experimental measurements of $T_{g,1}$ and $T_{g,2}$ fit well with the predicted ones using the Fox equation for both systems. Overall, with the increase of the thiol-epoxy ratio, $T_{g,1}$ increases while $T_{g,2}$ decreases. $T_{g,1}$ arises from the formation of a moderately crosslinked network structure (thiol-epoxy polymerization) and the presence of unreacted epoxy groups (see Figure 1), while $T_{g,2}$ adds a highly densely crosslinked network given by the epoxy homopolymerization and all functional groups have reacted (see Figure 2). The materials with a low thiol:epoxy ratio have little contribution from the thiol-epoxy polymerization and a high contribution from the epoxy homopolymer network, hence the lower $T_{g,1}$ and higher $T_{g,2}$. In contrast, materials with a high thiol:epoxy ratio have a higher contribution from the thiol-epoxy polymerization and lower contribution from the epoxy homopolymer network, hence the higher $T_{g,1}$ and the little increase up to $T_{g,2}$. As it is well-known, the $T_g$ of thermosets mainly depends on the network structure hindrance and crosslinking density in such a way that, the higher the $T_g$ due to highly crosslinked and physically hindered network structures, the broader the relaxation process and the stronger the effect on the mechanical properties (brittle materials). This is of high relevance when defining the operational design of the final material. Depending on the application, i.e. coatings, actuation purposes or structural applications, the final material should have specific thermal and mechanical properties. A number of useful parameters such as the storage modulus in the relaxed state of the network, the FWHM (full width at half maximum) and *tanδ* peak values are an indication of the crosslinking density and the heterogeneity of the network structure. In Figure 13, the relaxed modulus, as well as both, the FWHM and *tanδ* peak values are represented for the different thiol-epoxy ratios of study. In addition, the $T_{g,2}$ is shown to facilitate the comparison between materials. As it is observed, high values of $T_{g,2}$ (low thiol-epoxy ratios) lead to high values of $E_r$ and more heterogeneous

network structures (higher FWHM and lower *tanδ* peak values), whereas lower values of $T_{g,2}$ (increasing the thiol-epoxy ratio), lead to lower values of $E_r$ and more homogeneous network structures.

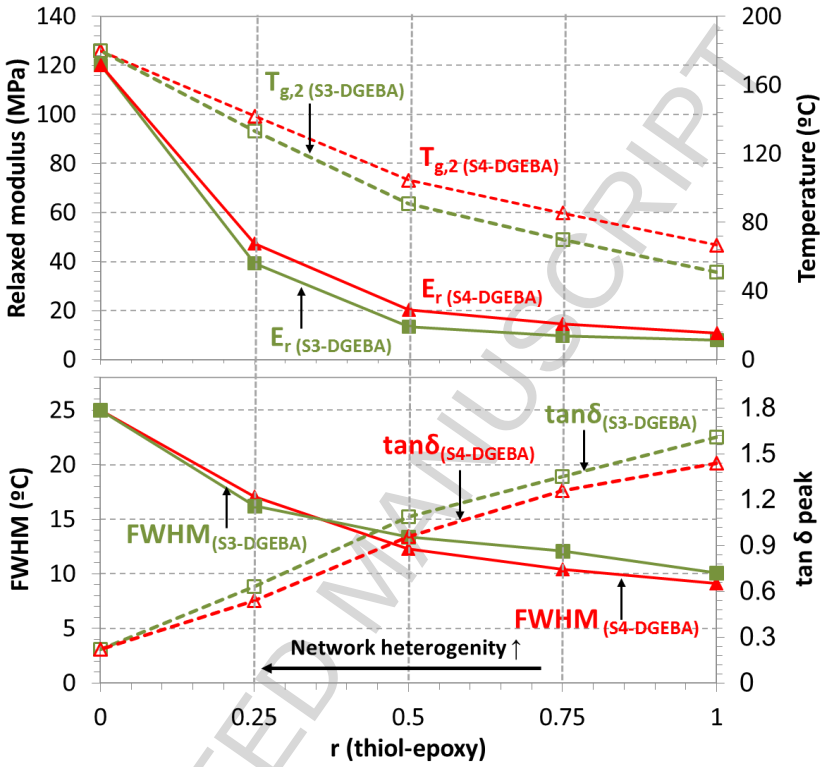


**Figure 13.** Analysis of the network structure properties (heterogeneity, crosslinking density and relaxed modulus) in both systems, S3-DGEBA and S4-DGEBA.

Taking into account the different $T_{g,1}$, $T_{g,2}$ and the rheological properties of the intermediate materials depending on the thiol-epoxy ratio, the graphic in Figure 12 can be divided in two sections as previously explained: section (A), from $r$ = 0 (DGEBA homopolymerization) to $r_d$ (no-dripping/critical ratio), section (B), from $r_d$ to the stoichiometric ratio. In section (A), the intermediate material is liquid-like and the viscosity increases with increasing the ratio. The final material shows moderate to high $T_g$ values (from 60 to 180°C depending on the system and the stoichiometric ratio), but may show low impact resistance and higher fragility when the ratio is too close to "0" because of the high content of unreacted epoxy groups forming a highly crosslinked network structure [29]. This type of materials could be of high interest in applications such as adhesives or primer coatings with high temperature resistance, given the good adhesion of the liquid-like intermediate material (see in Figure 3) and the high $T_g$ achieved in the final material, or else in applications where the intermediate flowing ability can be controlled or else is irrelevant, such composites or moulded compounds that are processed in one or two stages. In the vicinity of the critical ratio, the final materials show homogeneous network structures and sufficiently low $E_r$ values (see Figure 13) in comparison with materials in section (B), which make them promising in terms of mechanical elongation and strength. The intermediate materials at room temperature behave solid-like and have high conformability (with $T_{g,1}$ values around 20°C and sufficiently low modulus to reach high elongation, see examples in Figure 4) and the final materials still show well-separated $T_g$ values (from 20°C in the intermediate material to 65-90°C in the final material). The final shape may

not be well-retained below this critical ratio due to the significant elongation during the second curing stage, but applications in which films are required or when a mould is used, can perfectly fit with these materials.

In section (B) the increase in $T_g$ between the intermediate and final stages is more limited, especially as the thiol-epoxy ratio approaches 1. The materials are completely able to retain the imposed final shape but they are hardly processed with increasing the thiol-epoxy ratio. Actually, increasing the ratio worsens the conformation but increases $T_{g,1}$, in such a way that the intermediate material can be exploited for shape-memory applications, i.e. the S4-DGEBA-0.80 has 42°C of $T_{g,1}$ and 66°C of $T_{g,2}$ (still separated temperatures to consider them two different materials). Such applications include fold-deploying materials to reduce the volume in storage or transport stages [35]. Furthermore, the shape-memory capability can be used to impose an uncommon complex temporary shape which further will be fixed into a permanent shape through the second curing stage by simply fastening it externally impeding the shape-recovery effect. An example of the fold-deploying and further fixation of a complex shape is shown in Figure 14. As it is observed, the intermediate material is easily processed into different reduced temporary-shapes, and the original shape can be recovered through the shape-memory effect at low temperature (avoiding the triggering of the second curing stage). After that, a semi-tube shape (for example) can be imposed again through a shape-memory programming process and further fixed through the second curing stage.

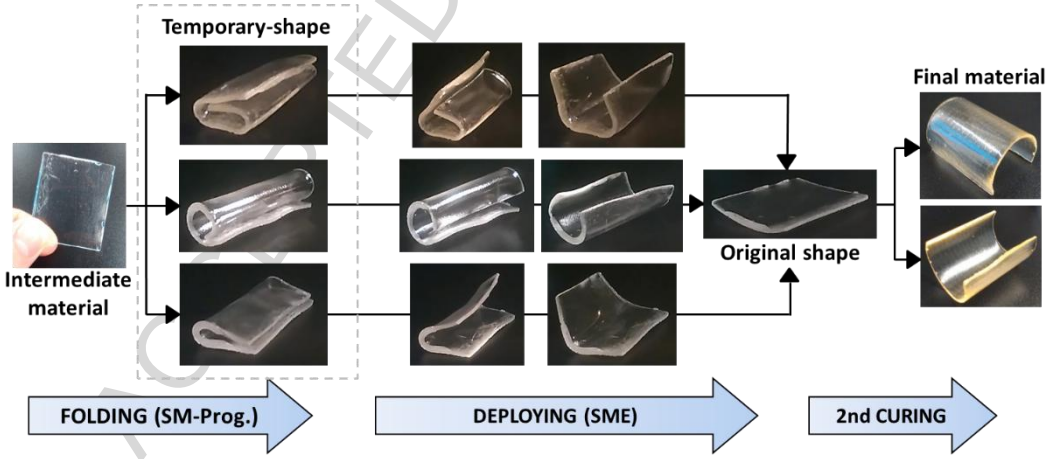


**Figure 14.** Example of fold-deploying and further shape-fixing application taking advantage of the shape-memory capability of the intermediate material in formulation S4-DGEBA-0.8.

In general, all final materials above the critical ratio are promising in shape-memory applications: the possibility to obtain uncommon shaped final materials (see Figure4) and the tailoring capability of the network structural properties (from high to moderately low $E_r$ values with relatively homogeneous relaxation processes) makes them suitable materials.

## 4. Conclusions

Sequential dual-curing of off-stoichiometric thiol-epoxy mixtures has been successfully achieved by using thiol compounds of different functionality and specific curing conditions. Appropriately choosing the thiol-epoxy ratio (higher than the critical ratio, $r_c$), solid-like and conformable intermediate materials have been obtained after the first curing stage. Temporary shapes can be easily produced and fixed by crosslinking taking place during the second curing stage. Nevertheless, some troubles fixing the final shape were found when using formulations close to the theoretical $r_c$: after the second curing stage, completely or partially losing of the imposed shape was appreciated in form of drops or elongation of the sample (dripping behaviour). Through a visual study of this phenomenon, $r_c$ has been found higher than expected, pointing out that probably the gelation is taking place at higher conversion than expected. DSC analysis of different parts in the tested samples evidenced that the sample structure remains homogeneous after the second curing stage and therefore no flow of unreacted species is taking place but the whole sample suffers an irreversible elongation.

The rheological analysis verified that, as stated above, gelation takes place at higher conversion than the predicted from the theory applied. In formulations where dripping was appreciated, the cross of the $\delta$ curves does not take place until the second curing stage is triggered, whereas at a certain thiol-epoxy ratio (called "no-dripping" ratio, $r_d$) the crossing is well-appreciated during the first curing stage. Moreover, the storage modulus dramatically decreases to a minimum value during the temperature increase from 50°C to 120°C in the second curing stage that, in the case of samples where "dripping" was appreciated, reaches compromising values that could produce such elongation caused by the own weight of the sample.

The $T_g$ of the intermediate and final materials can be obtained from the application of the Fox equation using the initial and final $T_g$'s of the different components. Plotting these glass transitions against the thiol-epoxy ratio, as well as the effective critical ratio, is a useful tool for the analysis of the applicability of the different materials. Possible applications can be defined on the basis of this critical ratio, taking advantage of the flowing ability, the high deformability or the shape-memory properties of the intermediate materials. Final material with tuneable properties can be achieved: from moderately crosslinked to highly densely crosslinked network structures with $T_g$ ranging from 40°C (at high thiol-epoxy ratios) up to 180°C (at low thiol-epoxy ratios) only using two different thiol-epoxy systems. This evidences the potential capability of this system to produce tailor made materials through the use of different thiol and epoxy compounds.

## Acknowledgements

The authors would like to thank MICINN (MAT2014-53706-C03-01 and MAT2014-53706-C03-02) and Generalitat de Catalunya (2014-SGR-67) for financial support.

## References


[1] JP. Pascault, H. Sautereau, J. Verdu, RJJ. Williams, Thermosetting Polymers. 1st edn. CRC Press; New York.**2002**.

[2] RJ. Sheridan, CN. Bowman.Understanding the process of healing of thermoreversible covalent adaptable networks, Polym Chem **2013**; 4: 4974-4979. DOI: 10.1039/C2PY20960H.

[3] CJ. Kloxin, CN. Bowman.Covalent adaptable networks: smart, reconfigurable and responsive network systems. Chem Soc Rev**2013**, 42:7161-73. DOI:10.1039/c3cs60046g.

[4] A. Lendlein. Progress in actively moving polymers. J Mater Chem **2010**;20:3332-3334.DOI: 10.1039/C004361N.

[5] BD. Mather, K. Viswanathan, KM. Miller, TE. Long. Michael addition reactions in macromolecular design for emerging technologies. Prog Polym Sci **2006**;31(5):487-531.DOI: 10.1016/j.progpolymsci.2006.03.001.

[6] C. Decker, F. Masson, R. Schwalm. Dual-curing of waterborne urethane-acrylate coatings by UV and thermal processing. Macromol Mater Eng **2003**;288(1):17-28.DOI: 10.1002/mame.200290029.

[7] S. Simić,B: Dunjić, S. Tasić, B.Božić,D. Jovanović, I. Popović. Synthesis and characterization of interpenetrating polymer networks with hyperbranched polymers through thermal-UV dual curing. Prog Org Coatings **2008**;63(1):43-48. DOI:10.1016/j.porgcoat.2008.04.006.

[8] DP. Nair, NB. Cramer, JC: Gaipa, MK. McBride, EM. Matherly, RR. McLeod, R. Shandas, CN. Bowman.Two-Stage Reactive Polymer Network Forming Systems. Adv Funct Mater **2012**;22(7):1502-1510. DOI: 10.1002/adfm.201102742.

[9] Q. Lian, Y. Li, T. Yang, K. Li, Y. Xu, L. Liu, J. Zhao, J. Zhang, J. Cheng. Study on the dual-curing mechanism of epoxy/allyl compound/sulfur system J Mater Sci **2016**;51(17):7887-7898.DOI: 10.1007/s10853-016-0044-z.

[10] C. Acebo, X. Fernández-Francos, X. Ramis X, À. Serra. Multifunctional allyl-terminated hyperbranched poly(ethyleneimine) as component of new thiol–ene/thiol–epoxy materials. React Funct Polym **2016**;99:17-25. DOI:10.1016/ j.reactfunctpolym.2015.12.003.

[11] D. Guzmán, X. Ramis, X. Fernández-Francos,À. Serra. Preparation of click thiol-ene/thiol-epoxy thermosets by controlled photo/thermal dual curing sequence. RSC Adv **2015**;5:101623-101633.DOI: 10.1039/c5ra22055f.

[12] G. González, X. Fernández-Francos, À. Serra, M. Sangermano, X. Ramis. Environmentally-friendly processing of thermosets by two-stage sequential aza-Michael addition and free-radical polymerization of amine–acrylate mixtures. Polym Chem **2015**;6: 6987-6997. DOI: 10.1039/c5py00906e.

[13] RA. Ortiz, AEG. Valdéz, LB. Duarte, RG. Santos, LRO. Flores, MD. Soucek.Development and study of a coupling agent for photocurable hybrid thiol/ene/cationic formulations. Macromol Chem Phys **2008**;209(20):2157-2168.DOI: 10.1002/macp.200800305.

[14] HC. Kolb,MG. Finn,KB. Sharpless. Click Chemistry: Diverse Chemical Function from a Few Good Reactions. Angew Chem Int Ed. **2001**;40(11):2004-2021.

[15] JE. Moses, AD. Moorhouse. The growing applications of click chemistry. Chem Soc Rev **2007**;36:1249-1262.DOI: 10.1039/B613014N.

[16] WH. Binder, R. Sachsenhofer. "Click" chemistry in polymer and materials science. Macromol Rapid Commun **2007**;28(1):15-54.DOI: 10.1002/marc.200600625.

[17] CE. Hoyle, AB. Lowe, CN. Bowman. Thiol-click chemistry: a multifaceted toolbox for small molecule and polymer synthesis. Chem Soc Rev **2010**;39:1355–87. DOI: 10.1039/b901979k.

[18] J. Shin, H. Matsushima, CM. Comer, CN. Bowman, CE. Hoyle. Thiol-isocyanate-ene ternary networks by sequential and simultaneous thiol click reactions. Chem Mater **2010**;22(8):2616-2625. DOI:10.1021/cm903856n.

[19] DP. Nair, M. Podgórski,S. Chatani, T. Gong, W. Xi, CR. Fenoli, CN. Bowman. The Thiol-Michael addition click reaction: A powerful and widely used tool in materials chemistry. Chem Mater **2014**;26(1):724-744. DOI: 10.1021/cm402180t.

[20] A. Brändle, A. Khan. Thiol–epoxy "click" polymerization: efficient construction of reactive and functional polymers. Polym Chem **2012**;3:3224.DOI: 10.1039/C2PY20591B.

[21] K. Jin, WH. Heath, JM. Torkelson. Kinetics of multifunctional thiol-epoxy click reactions studied by differential scanning calorimetry: Effects of catalysis and functionality. Polymer **2015**;81:70-78.DOI: 10.1016/j.polymer.2015.10.068.

[22] RM. Loureiro, TC. Amarelo, SP. Abuin, ER. Soulé, RJJ. Williams. Kinetics of the epoxy-thiol click reaction initiated by a tertiary amine: Calorimetric study using monofunctional components. Thermochim Acta **2015**;616:79-86.DOI:10.1016/j.tca.2015.08.012.

[23] X. Fernández-Francos, AO. Konuray, A. Belmonte, S. De la Flor, À. Serra, X.Ramis. Sequential curing of off-stoichiometric thiol–epoxy thermosets with a custom-tailored structure. Polym Chem **2016**;7:2280-2290.DOI: 10.1039/C6PY00099A.

[24] MS. Heise, C. Martin. Curing Mechanism and Thermal Properties of Epoxy-Imidazole Systems. Macromolecules **1989**;22(1):99-104.DOI: 10.1021/ma00191a020.

[25] S. Vyazovkin, N.Sbirrazzuoli. Mechanism and Kinetics of Epoxy-Amine Cure Studied by Differential Scanning Calorimetry. Macromolecules **1996**;29(6):1867-1873.DOI: 10.1021/ma951162w.

[26] R. Sengupta, S. Chakraborty, S. Bandyopadhyay, S. Dasgupta, R. Mukhopadhyay, K. Auddy, AS. Deuri. A Short Review on Rubber/Clay Nanocomposites with Emphasis on Mechanical Properties. Engineering **2007**;47(11):21-25. DOI: 10.1002/pen.20921.

[27] D. Guzmán, X. Ramis, X. Fernández-Francos, À. Serra. New Catalysts For Diglycidyl Ether of Bisphenol A Curing Based on Thiol-Epoxy Click Reaction. Eur Polym J **2014**;59:377-386. DOI:10.1016/j.eurpolymj.2014.08.001.

[28] X. Lu, RA. Weiss. Relationship between the glass transition temperature and the interaction parameter of miscible binary polymer blends. Macromolecules. **1992**;25(12):3242-3246.DOI: 10.1021/ma00038a033.

[29] DC. Timm, AJ. Ayorinde, RF. Foral. Epoxy mechanical properties: function of crosslink architecture. Poylm Int**1985**;17(2):227-232.DOI: 10.1002/pi.4980170226.

[30] M. Shimbo, M. Ochi, Y. Shigeta. Shrinkage and internal stress during curing of epoxide resins. J Appl Polym Sci **1981**;26(7):2265-2277.DOI: 10.1002/app.1981.070260714.

[31] D. Santiago, A. Fabregat-Sanjuan, F. Ferrando, S. De la Flor. Recovery stress and work output in hyperbranched poly(ethyleneimine)-modified shape-memory epoxy polymers. J Polym Sci Part B Polym Phys **2016**;54:1002-1013.DOI:10.1002/polb.24004.

[32] Y. Tanaka, JL. Stanford, R. Stepto. Interpretation of Gel Points of an Epoxy-Amine System Including Ring Formation and Unequal Reactivity: Reaction Scheme and Gel-Point Prediction. Macromolecules. **2012**;45(17):7186-7196.DOI:10.1021/ma300984u.

[33] Y. Tanaka, JL. Stanford, R. Stepto. Interpretation of Gel Points of an Epoxy-Amine System Including Ring Formation and Unequal Reactivity: Measurements of Gel Points and Analyses on Ring Structures. Macromolecules. **2012**; 45(17): 7197-7205. DOI: 10.1021/ma3009838.

[34] A. Pizzi. Principles of Polymer Networking and Gel Theory in Thermosetting Adhesive Formulations. In Handbook of Adhesive Technology.2nd edn.Marcel Dekker Inc; New York,**2003**.

[35] A. Belmonte, D. Guzmán, X. Fernández-francos X, S. De la Flor. Effect of the Network Structure and Programming Temperature on the Shape-Memory Response of Thiol-Epoxy " Click " Systems Polymers **2015**;7(10):2146–64. DOI:10.3390/polym7101505.

Graphical abstract

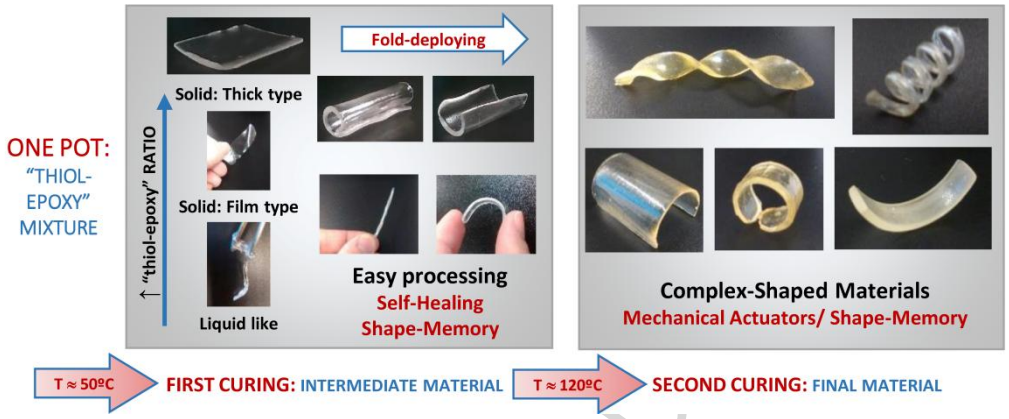

Highlights

- Multifunctional materials are developed with a sequential dual-curing system based on off-stoichiometric “thiol-epoxy” mixtures by using thiol compounds of different functionality.
- By appropriately choosing the “thiol-epoxy” ratio, it is possible to develop solid-like and conformable intermediate materials for challenging processing scenarios.
- Uncommon- and complex-shaped final materials, such as, plaited- or spring- shaped materials, can be obtained.
- The material’s physical and thermomechanical properties can be easily tailored by changing the “thiol-epoxy” ratio to optimise their performance and applicability.
- These materials can be used in a wide range of shape-memory applications or in the development of complex mechanical actuators.